Semiconductor Physics, Quantum Electronics & Optoelectronics. 2003. V. 6, N 3. P. 287-293.

PACS: 63.22.+m, 72.10.Di, 78.30.–j

Resonance Raman scattering by intersubband plasmon-phonon excitations in InAs/AlSb structures

M.Ya. Valakh[1], V.V. Strelchuk[1], O.F. Kolomys[1], H.L. Hartnagel[2], J. Sigmund[2]

[1] *Institute of Semiconductior Physics, NAS of Ukraine, 03028 Kyiv, Ukraine*

[2] *Institut für Hochfrequenztechnik, Fchberreich Electrotechnik und Informationstechnik, TU Darmstadt, Merckstr. 25, 64237 Darmstadt, Germany*

Abstract. Intersubband plasmon-phonon excitations in InAs/AlSb with InSb- and AlAs-like interfaces were studied using the Raman scattering method. It was found that InSb interface is characterized by a decreasing concentration and increasing mobility of 2D electrons in InAs quantum wells. In the case of AlAs interface at the heterojunction quantum well – barrier, the formation of $AlSb_{1-x}As_x$ solid solution takes place. Revealed are considerable concentration changes for 2D electrons at low temperatures in dependency on the excitation quantum energy.

Keywords: heterostructure, plasmon-phonon excitations, resonance Raman scattering.

Paper received 16.05.03; accepted for publication 17.06.03.

1. Introduction

In the course of formation of semiconductor heterostructure properties, physical-and-chemical properties of heterostructure constituents, especially differences in their lattice parameters, play a leading role. There exist only several systems with close values of lattice parameters. Fig. 1 shows the dependency of low-temperasture band gap widths on the lattice parameter for some semiconductor compounds. Choosing the necessary heteropair, one can create heterostructures with the preliminary set band separation value or quantum wells (QW) with a given potential profile, i.e., realize the main idea of the so-called "zone engineering". Among A^3B^5 compounds with the close values of lattice parameters, the classical heteropair GaAs/AlAs is the most thoroughly studied.

In recent years, actively studied is one more family of compounds creating practically non-strained pairs. It is the so-called "6.1 A family" including InAs, GaSb, AlSb. Heterostructures based on these compounds are used in optoelectronic devices applied in the near- and mid-infrared spectral ranges and using interband optical transitions.

The nearly-lattice-matched InAs/AlSb heterostructures (a_{InAs} = 6.0584 Å, a_{AlSb} = 6.1355 Å), the very large conduction band offsets of 1.367 eV between Γ conduction band minimum in InAs and the X conduction band minimum in AlSb (Fig. 2), combined with a low effective mass of electrons in InAs ($0.023m_0$, compared to $0.067m_0$ in GaAs and $0.19m_0$ in Si) are attractive for possible devices such as high-speed field-effect transistors (HEMT) [1], hetero-barrier varactors [2], resonant-tunneling diodes (RTD) [3], as well as for spintronic applications [4,5].

Electron transport measurements show that structures with 15 nm InAs width have 2D electron concentration about 10^{12} cm^{-2} and the electron mobilities at low temperatures reaching $2\cdot10^5$ cm^2/V·s [6–8].

InAs/AlSb QWs exhibit several unique properties that distinguish them from the thoroughly investigated GaAs-$Al_xGa_{1-x}As$ heterostructures. In particular, electron densities above 10^{12} cm^{-2} can be achieved without intentional doping and are strongly dependent on sample structure detailes, namely: AlSb barrier thickness as well as upper protective GaSb layer that prevents AlSb oxidation [8]. Identified are three main sources of these electrons: donor states on the surface of the protective GaSb layer, deep donor states in AlSb barriers (as the result of "antisite

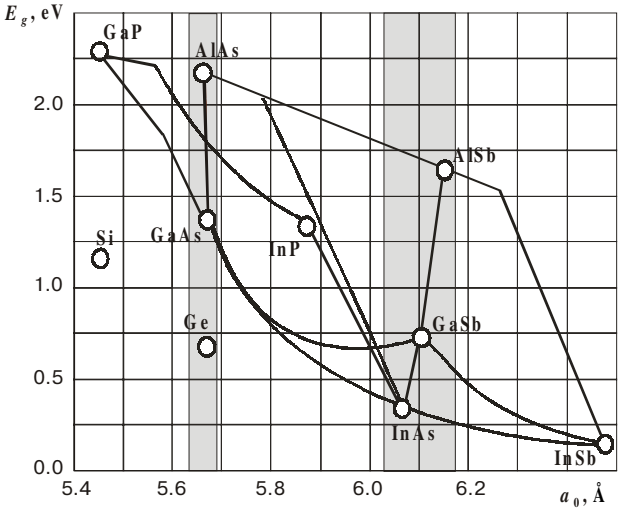

Fig. 1. Band gap energy E_g versus lattice parameter a_0 for various III-V semiconductors, Si and Ge.

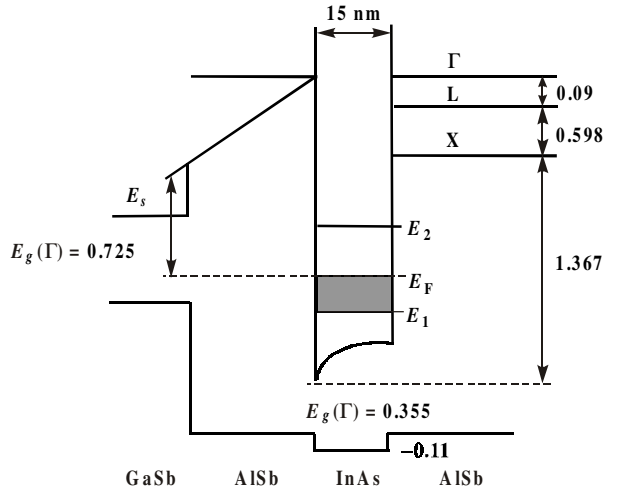

Fig. 2. Energy band structure of GaSb/AlSb/InAs/AlSb heterostructures.

doping", when As atoms occupy Al sites) and interface donor states at InAs-AlSb interfaces [8,9]. When the thickness of the upper AlSb barrier are less than 50 nm, the dominating contribution into the concentration of 2D electrons in InAs QWs is provided by surface donor GaSb states [9]. Antisite defects in the barrier layers are expected to act as a source of additional free electrons [8]. In the latter case, 2D electron gas in InAs QW may be formed due to the charge carriers transferred from the "antisite" donors of AlSb layer into the energetically lower conduction band of the InAs layer, giving rise to depletion of the electrons in AlSb layers and to accumulation in the InAs layer.

It is ascertained that electrical [8] and optical [10] properties of InAs/AlSb superlattices are strongly dependent on the bond type at the interface between InAs QW and AlSb barrier.

Really, the InAs/AlSb system has a feature that differs it markedly from the GaAs/ (Al,Ga)As. Because both the cation and anion change across InAs/AlSb interface, two distinctly different interface structures can be obtained (Fig. 3). In one case, InAs would be terminated with a final layer of In, and the adjoining AlSb would start with a layer of Sb, which results in appearance of InSb bonds across the interface. This is the so-called "InSb-like" interface. The complement to it is the "AlAs-like" interface, where Al atoms from AlSb side are bound to As atoms at InAs side. Also, the alternative InSb/AlAs interface can be grown. The high level of control provided by the molecular-beam epitaxy (MBE) method should make it possible to grow structures with these interfaces [8].

In [11,12] resonant inelastic light scattering was proposed as a spectroscopic tool for the study of the elementary excitations of quasi-two-dimensional electron systems in semiconductors. Of special interest are the investigations of the resonance behavior of mixed plasmon-phonon modes under excitations near optical gaps nonrelated with electron-filled states. It is especially important in the case of semiconductors with small energy gaps, such as InAs and AlSb, where optical gaps E_0 and $E_0 + \Delta_0$ are difficult to practically investigate using resonance Raman scattering. There are only a few reports on intersubband Raman scattering in InAs/AlSb [13-15], InAs/GaSb [16] QWs and investigation of interface quality in InAs/AlSb [17].

In this work investigated are mixed intersubband plasmon-LO-phonon excitations in InAs/AlSb structures with InAs QWs of 15 and 32 nm thickness on dependency on the type of interface bonds as well as technology of their realization.

Variations of the Raman signal with laser energy due to different resonance behaviors of the contributing scattering mechanisms and changes in the penetration depth of the laser photons were investigated and analyzed.

2. Experimental details

The unintentionally doped QW structures were grown on semi-insulating (100) GaAs substrates in Riber 32 molecular-beam epitaxy (MBE) with a valved cracker cell for arsenic and a standard cracker cell for antimony to generate molecular beams of As_2 and Sb_2. For the quantum well growth, including the barriers and cap layer, the substrate temperature was 435 °C to reduce intermix-

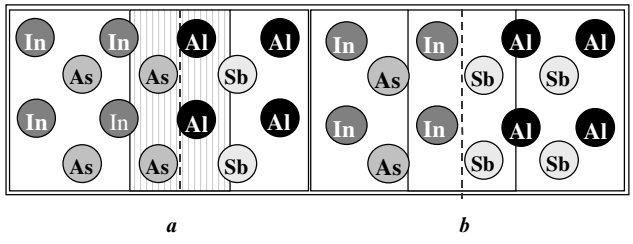

Fig. 3. Interface structures for the (*a*) AlAs-like interface and (*b*) InSb-like interface.

ing at the interface. The nominal thickness of AlSb barrier was 24 nm and InAs QW layer was 15 nm or 32 nm. To protect AlSb from reaction with water vapour in the air, 4.8 nm GaSb cap layer was grown on the top of the structure. In more detail, growing the quantum well structures will be described elsewhere [6,7].

Structures possessed two types of interfaces between InAs and AlSb layers: AlAs- and InSb-like ones. In the latter case, the samples were grown with and without stopping MBE process at QW interface. As shown in [6], this additive interruption of MBE process results in the decreasing density of structural defects, at least, of the electrically active ones determining 2D electron concentration in InAs QWs, and in noticable growth in the carrier mobility.

The Raman experiments were performed in typical near-backscattering geometry from the (100) growth plane. As the excitation sources, different lines of of Ar^+ laser with an input power lower than 20 mW were used. The laser beam was focused into a spot size approximately 100 μm in diameter. Raman spectra were measured at 300 and 90 K. The scattered light was analyzed using a double monochromator (DFS-24) with photon counting system for detection. Laser plasma line frequencies were used to check the precise phonon line position.

3. Results and discussion

Fig. 4 represents Raman spectra of the InAs QW sample with the thickness 15 nm and InSb interface in back-scattering geometry relatively to (100) plane under excitation (E_{exc} = 2.54 eV) close to the resonance with the optical gap E_1 InAs equal to 2.49 (2.61) eV at T = 300(80) K [18]. Polarizations of incident and scattered light were set in parallel $z(x, x)\bar{z}$ and perpendicular $z(x, y)\bar{z}$ configurations. As far as non-resonant excitation conditions take place for AlSb barrier layers, Raman spectra were normalized to the intensity of LO(AlSb) mode $\nu_{LO(AlSb)} \approx$ 340.4 cm^{-1}.

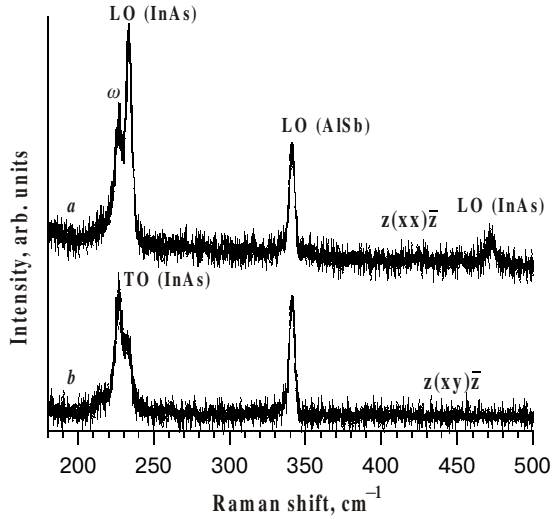

Fig. 4. Raman spectra recorded at 300 K under 2.54 eV excitation for the structures InAs/AlSb.

Besides LO(AlSb) band, in the spectrum one can observe two clearly pronounced peaks in the range 220–240 cm^{-1}. The low-energy one is caused by the low-frequency mixed intersubband plasmon-LO-phonon mode of InAs QW ($\omega \approx 228.4\ cm^{-1}$), while the high-energy one – by the non-screened LO-phonon mode of InAs ($\omega_{LO(InAs)} \approx$ $\approx 234.4\ cm^{-1}$) [18]. In addition, in $z(x, x)\bar{z}$ spectrum registered is a clear peak close to 472 cm^{-1} corresponding to the two-phonon 2LO(InAs) mode (Fig. 4a). A small contribution into LO(InAs) band can be provided by the scattering on LO(GaSb)-phonons of the protective layer. We observed the respective peak of LO(GaSb) mode at T = = 90 K and resonance excvitation near the optical gap E_1 in GaSb (E_{exc} = 2.71 eV).

It is known that in polarized spectra [$z(x, x)\bar{z}$] intrinsic two-LO phonon scattering is allowed, whereas one-LO-phonon scattering caused by the deformation potential mechanism is forbidden through symmetry reasons. For resonant excitation, however, intrinsic one-LO-phonon scattering via the Froelich mechanism, as well as defect-induced one-LO-phonon scattering, contribute to the Raman spectrum [19]. Therefore, the presence of an InAs two-LO-phonon signal, and the observation that InAs one-LO-phonon scattering is stronger for parallel than for crossed polarizations, show clearly the resonant enhancement of LO-phonon scattering from the InAs quantum well [18]. The non-resonantly excited AlSb one-LO-phonon signal, in contrast, is, as expected [19], a most intensive for crossed polarizations. In addition, the Raman spectrum shows a weak peak at 218 cm^{-1} that is assigned to scattering by the transverse InAs mode forbidden in this configuration. Its appearance can be caused by presence of structural disorders in InAs QW.

Frequences of mixed intersubband plasmon-phonon modes in the doped QW are determined from the condition that the real part of the dielectric function $\varepsilon(\omega)$ is equal to zero. It is assumed that only the main subband is filled with electrons (which is usually valid in experiments), and transitions between the first excited and main subbbands take place. Than, in the approximation of small wave vectors $(\vec{q} \approx 0)$ [11,20]:

$$\omega_{\pm}^2 = \frac{1}{2}\left(\omega_{01}^2 + \omega_{LO}^2 + \omega_P^{*\,2}\right) \pm$$
$$\pm\frac{1}{2}\left[\left(\omega_{01}^2 + \omega_{LO}^2 + \omega_P^{*\,2}\right)^2 - \right.$$
$$\left. -4\left(\omega_{01}^2\omega_{LO}^2 + \omega_{TO}^2\omega_P^{*\,2}\right)\right]^{1/2} \qquad (1)$$

where ω_{TO} is TO-phonon frequency, ω_{01} – the intersubband splitting between the first excited and main subbands, ω_P^* – the effective plasma frequency: $\omega_P^{*\,2} = \frac{2 n_S \omega_{01}}{\hbar} V_{01}$, V_{01} – the Coulomb matrix element of interaction between the main and excited subbands of QW [21].

It should be noted that the equation (1) is deduced in the approximation of small wave vectors, for which single-particle excitations are impossible, that is without taking the Landau decay into account.

Energies of intersubband excitations are shifted into the high-energy side due to the depolarization effect by the value [22,23]:

$$\omega_{01}^{*\,2} = \omega_{01}^2 + \omega_P^{*\,2} \qquad (2)$$

It follows from the equation (1) that $\omega_{\pm}$ depends on both values ω_{01} and ω_P^*, that is, on the well thickness and electron density.

When $\omega_{01} >> \omega_{LO}$ ($\omega_P^* >> \omega_{LO}$), the high-frequency mode possesses a plasmon-like character and $\omega_+ \approx \omega_P^* >> \omega_{LO}$, while the low-frequency phonon-like mode ω_- may be considered as a strongly screened LO phonon, frequency values of which are changed from ω_{LO} (non-screened LO phonon) to ω_{TO} (fully screened LO phonon).

In InAs/AlSb structure with InAs QW of 15 nm thickness, $\omega_{01} >> \omega_{LO}$ and $\omega_P^* >> \omega_{LO}$ [15]. Consequently, in the Raman spectra (Fig. 4) ω_- mode should give its contributiion into the frequency range $\omega_{TO} \le \omega_- \le \omega_{LO}$. In investigated structures, ω_+ mode was observed at $\omega_+ \approx 1050\text{cm}^{-1}$ [15]. This situation is realized in our case, too. However, contrary to [15], we have not found ω_+, which can be caused by both the other experiment geometry and considerable Landau decay determined by the finite temperature value as well as effects of collision widening.

The experimentally observed LO(InAs) frequency value ($\omega_{LO(\text{InAs})} \approx 234.4\ \text{cm}^{-1}$) is less than the respective value characteristic for the bulk InAs ($\approx 238.6\ \text{cm}^{-1}$ [18]). This low-frequency shift can arise due to effects of phonon confinement and lateral expansion tensions.

Longwave optical phonons in InAs and AlSb are localized in respective heterostructure layers InAs/AlSb as a consequence of a considerable energy difference in their dispersion dependences in all the wave vector range [24]. Therefore, the low-frequency LO-phonon shift will be determined by their dispersion (scattering wave vector $k = \pi/d$), i.e., by the finite thickness (d) of InAs (AlSb) layer. Our estimations showed that in the case this shift does not exceed $\sim 0.02\ \text{cm}^{-1}$. It can be reliably registered only at $d_{\text{InAs}} < 3$ nm [25].

In InAs realized are low lateral expansion tensions caused by some mismatch of lattice parameters in InAs and AlSb (~1.26 %), which results in the low-energy shift of LO(InAs) phonon. At under-critical thickness values of InAs layer (≤ 10.0 nm [26]), the magnitude of this shift estimated from the expression [27]

$$\Delta\omega_{\text{strain}}(LO) = -330.9\varepsilon,$$

is ~ 4.2 cm^{-1}, which coincides with the experimentally observed one.

Thus, the performed analysis of possible reasons determining the shift of LO(InAs) phonons showed that the effect of tension is the dominating one.

Also investigated were InAs/AlSb structures with the thickness of InAs QW 32 nm and InSb interfaces. As seen from Fig. 5, the intensity of LO(InAs) mode in the parallel polarization configuration $[z(xx)\bar{z}]$ is larger than that of ω_- mode, while in the perpendicular configuration $[z(x,x)\bar{z}]$ – the intensities of these modes are practically the same. The fact that for 32 nm QWs as compared to 15 nm ones we could observe sizable decreasing the intensities of LO(InAs) and ω_- modes accompanied with increasing their halfwidth is clearly indicative of worsening the structural quality of the probed InAs layer. Moreover, the position of ω_- mode is closer to the high-frequency side, and its increased halfwidth corresponds to decreasing the concentration and mobility of 2D electrons in InAs QWs. When exciting the sample in the non-resonant manner (Fig. 5, curve *c*), registered in the Raman spectrum are only LO(InAs) and LO(AlSb) bands. The absence of the low-frequency mixed ω_- mode betokens a strong resonance dependency of the latter on the excitation quantum energy.

To study influence of interface type InAs/AlSb structures and the procedure of interruped growth on the Raman spectra, we measured these structures at the nitrogen temperature and various excitation quantum energies. It is seen from Fig. 6 that the Raman spectrum of the structures studied depends both on the excitation quantum energy and technological specificity of their growing. These changes in spectra betoken a considerable differences in resonant dependences of mixed plasmon-phonon ω_- and LO(InAs) modes. An additional contribution into the observed changes can be caused by effects related to strong absorption of incident and scattered photons, which results in differences of wave vectors from $\vec{q}$ in the range of $\pm\,\text{Im}\{\vec{q}\}$ [28].

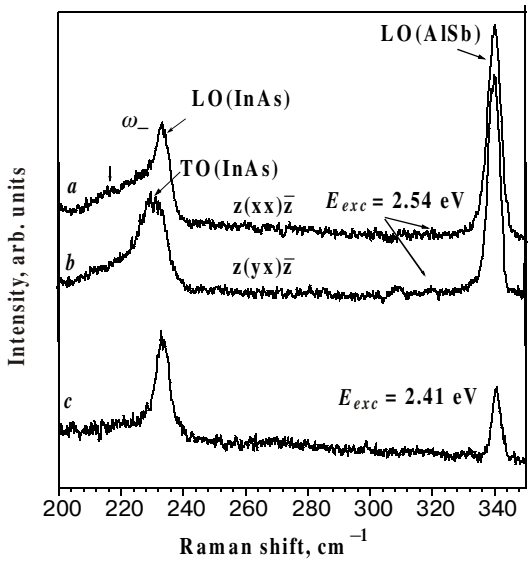

Fig. 5. Polarizational Raman spectra of InAs/AlSb structure with the nominal thockness of InAs QWs 32 nm and InSb interface (E_{exc} = 2.54 eV). The curve *c* corresponds to the non-polarized Raman spectrum (E_{exc} = 2.41 eV). T = 300 K.

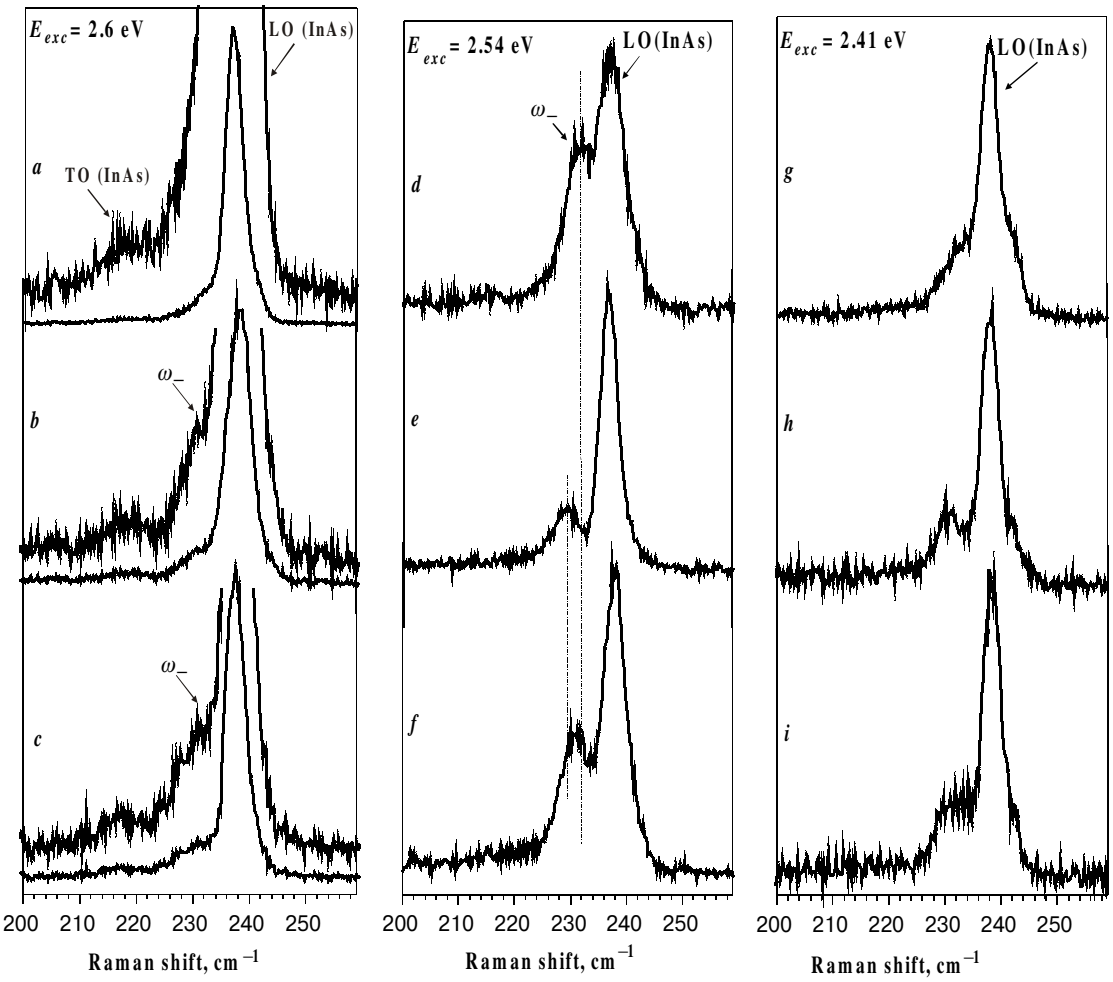

Fig. 6. Raman spctra of InSb/AlSb structures with the nominal thickness of InSb QWs 15 nm for InSb interfaces made using interruption of MBE growing process (curves *a*, *d*, *g*), and without it (curves *b*, *e*, *h*), as well as for AlAs interfaces with interruption (curves *c*, *f*, *i*). T = 90 K.

When E_{exc} = 2.6 eV (Fig. 5 *a,b,c*), we could observe an essential growth of LO(InAs) band intensity, which is conditioned by the proximity the excitation quantum energy to the optical gap E_1 in InAs (2.6 eV) [18]. Differences of the Raman spectra in the dependences on the interface type (Fig. 5 *a,c*) and the influence of InSb interface growing process interruption (Fig. 5*b*) can be interpreted by the following way. The absence of ω_- mode for the sample with InSb interface grown using the interruption method (Fig. 5, curve *a*) is caused by simultaneous action of two factors: i) the resonance amplification of the phonon component for the mixed plasmon-phonon ω_- and non-screened LO(InAs) modes as a result of the exact resonance with the gap E_1 in InAs; ii) decreasing 2D electron concentration in InAs QWs, which results in the high-frequency shift of ω_- mode. In the samples with InSb interfaces grown without growth interruption and with AlAs interfaces done using the interruption on interfaces (Fig. 5 *b, c,* respectively) ω_- mode is pronounced from the low-frequency side of LO(InAs) band. It corresponds to the increasing 2D electron concentration (the frequency of ω_- mode decreases) and to some removal from resonance excitation conditions for LO(InAs) mode. The latter is confirmed by the well-known fact of the essential growth in the energy E_1 in InAs ($\geq$ 200 meV) inherent to InAs/AlSb structures with AlAs interfaces as compared to those with InSb interfaces, which can be explained by different values of straines taking place at their heterointerfaces [29]. The above mentioned facts enable to assume that the strain value in InAs layer for structures with similar InSb interfaces depends not only on the interface type but on technological regimes of their growing. Straines are larger in the structures prepared without the growth interruption at the heterointerface. Besides, for all three samples we can clearly observe a weak scattering on TO phonons in InAs ($\approx$ 218 cm^{-1}) forbidden in the used experimental geometry.

The tendency of changing ω_- and LO(InAs) modes for these samples is more clearly pronounced in the Raman spectra at E_{exc} = 2.54 eV (Fig. 5 *d,e,f*). Seen is the considerable difference in ω_- intensity ratio. Energy positions of both ω_- and non-screened LO(InAs) mode are

changed, too. The highest intensity and the lowest halfwidth of ω_- mode are observed in the sample with InSb-like interface grown using the stop of epitaxy at the interface (Fig. 5*d*). The low-frequency shift of ω_- mode from 231.8 cm^{-1} (Fig. 5*d*) down to 231 cm^{-1} (Fig. 5*f*) and 229.2 cm^{-1} (Fig. 5*e*) betokens the increasing concentration of 2D electrons, and decreasing the intensity accompanied by increasing its halfwidth tells about the mobility drop [15,30]. Thus, our data confirm the mentioned after electrical investigations [6] fact of positive influence of the interrupted MBE process when growing InAs/AlSb heterostructures with InSb-like interfaces. As it was expected, the removal from the resonance excitation conditions results in essential decreasing the intensities of ω_- and LO(InAs) modes. However, it is noteworthy that the intensity of ω_- mode in the sample with InSb interface prepared without the growth interruption (Fig. 5*h*) is higher than that with it (Fig. 5*g*), which is sharply distinguished from the case E_{exc} = 2.54 eV (Fig. 5 *d,e*). The latter enables to assume that at E_{exc} = 2.41 eV the Raman spectrum can be contributed by non-homogeneities at the interface that can result in violation of the wave vector $\vec{q}$ conservation law. These non-homogeneities can be related to formation of $InAs_{1-x}Sb_x$ solid solutions as a result of interdiffusion, which was observed in InAs/AlSb multilayer structures [31]. The fact that these interdiffusion processes are less pronounced in the Raman spectra of the sample prepared without the growth stop is a good confirmation of our assumption. From this viewpoint, the non-homogeneities in structures with AlAs interfaces are the most possibly related to $Al_xIn_{1-x}As$ solid solution.

The more strange feature is pronounced from the high-frequency side of LO(InAs) band. Earlier, it was ascribed to GaAs interface vibrations [32–34]. It is possible only at presence of non-controlled As concentration excess in MBE growing chamber and its prevalable localization at the interfaces. To enlighten this question, it needs an additional investigation.

In Fig. 7*a*, in more detail, shown is the Raman spectrum at E_{exc} = 2.6 eV for the sample with InSb interface grown using growth interruption. The weak band corresponding to interface InSb-like vibrations is registered at ~190 cm^{-1} [17]. The other band at ~218 cm^{-1} is caused by the scattering on TO(InAs) phonons forbidden in this geometry. Both these facts seem to be very important. On the one hand, substantiated is the fact of the presence of a thin intermediate InSb layer at the boundaries of the quantum well. On the other hand, the indistinctness of the considered peak and appearance of the forbidden TO(InAs) one can be indicative of possible non-ideality of interface regions between QWs and barriers. Besides, the fact that 2LO(InAs) peak frequency (Fig. 7*b*) essentially exceeds the doubled LO(InAs) frequency value is indicative of considerable mixing the single-phonon LO vibrations with 2D electrons, which results in the low-frequency shift of the single-phonon LO(InAs) line.

Thus, we have demonstrated the efficiency of the resonance Raman spectroscopy method in investigations of 2D electron plasma and interface features in InAs/AlSb heterostructures. It has been shown that decreasing the concentration and increasing the mobility of 2D electrons in InAs quantum well take place in the case of InSb-like interface, these being especially pronounced when using the MBE method with interruption of the growing process at the interface. The resonance behavior of scattering intensities has been studied for the low-frequency mixed intersubband plasmon-LO-phonon ω_- mode and non-screened LO(InAs) mode when varying the excitation photon energy in the range of the resonance with the optical gap E_1 in InAs. For the first time, we found essential changes in 2D electron concentration and their interaction with LO(InAs) phonons in dependency on the excitation quantum energy at low temperatures. It is conditioned both by the proximity of the excitation quantum energy to respective optical gaps and by effects of polarization rule and wave vector conservation law disturbances.

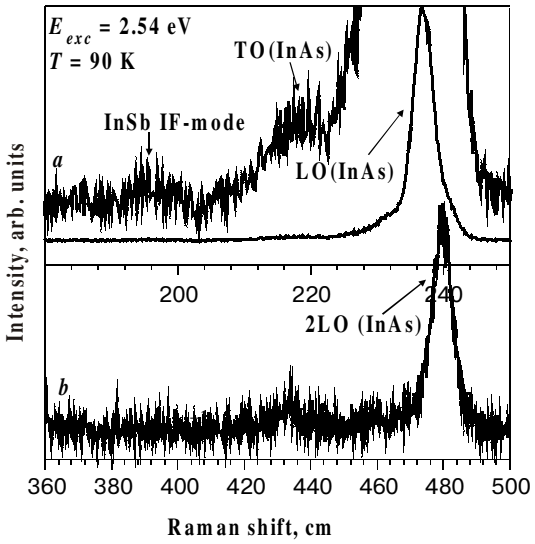

Fig. 7. Raman spectra of InAs/AlSb structure when the excitation nar the resonance with E_1 in InAs takes place. The frequency scale in the range of the first order LO (InAs) phonon (curve *a*) is doubled.

The work is fulfilled with the assistance of the Ukrainian-Russian program "Nanophysics and nanoelectronics". The authors thank V.G.Litovchenko for fruitful discussions.

References

1. W. Kruppa, J.B. Boss, B.R. Bennett, M.J. Yang // *Electron. Lett.*, **36**, p. 1888 (2000).
2. S.M. Nilsen, H. Groenqvist, H. Hjelmgreen, A. Rydberg, E.L. Kollberg // *IEEE Trans.Microwave Theory Tech.*, **41**, p. 572 (1993).
3. B.Z. Nosho, W.H. Weinberg, W. Barvosa-Carter, A.S. Bracker, R. Magno, B.R. Bennet, J.C. Culbertson, B.B. Shanabrook, L.J. Whitman // *J. Vac.Sci.Techn.*, **B17**, p. 1786 (1999).
4. P.R. Hammar, B.R. Bennett, M.J. Yang, M. Johnson // *Phys. Rev. Lett.*, **83**, p. 203 (1999).
5. D. Grundler // *Physics World April*, **2002**, p. 39, (2002).

6. J. Sigmund, M. Saglam, H.L. Hartnagel, V.N. Zverev, O.E. Raichev, P. Debray, G. Miehe, H. Fuess // *J. Vac. Sci. Techn.*, **B20**, p. 1174 (2002).
7. J. Sigmund, K. Karova, G. Miehe, M. Saglam, H.L. Hartnagel, H. Fuess // *I.Cryst.Growth*, **251**, p. 526 (2003).
8. G. Tuttle, H. Kroemer, J.H. English // *J. Appl. Phys.*, 67, p. 3032 (1990).
9. C. Nquyen, B. Brar, H. Kroemer, J.H. English // *Appl. Phys. Lett.*, 60, p. 1854 (1992).
10. J. Spitzer, A. Höpner, M. Kubal, M. Cardona, B. Jenichen, H. Neuroth, B. Brar, H. Kroemer // *J.Appl.Phys.*, **77**, p. 811 (1995).
11. E. Burstein, A. Pinczuk, D.L. Milles // *Surf. Sci.*, **98**, p. 451 (1980).
12. See, e.g., A.Pinczuk and G.Abstreiter, in *Light Scattering in Solids V*, edited by M.Cardona and G.Güntherodt (Springer, Berlin, 1989), p.153.
13. J. Wagner, J. Schmitz, D. Richards, J.D. Ralston, P. Koidl // *Solid-State Electronics*, **40**, p. 281 (1996).
14. J. Wagner, J. Schmitz, F. Fuchs, J.D. Ralston, P. Koidl, D. Richards // *Phys.Rev.*, **B51**, p. 9786 (1995).
15. D.Richards, J.Wagner, J.Schmitz // *Solid. State Commun.* // **100**, p. 7 (1996).
16. Y.B. Li, V.Tsoukawa, R.A. Stradling, R.L. Williams, S.J. Shung, I. Kamiya, A.G. Norman // *Semicond. Sci. Technol.*, **8** p. 2205 (1993).
17. I. Sela, C.R. Bolognesi, L.A. Samoska, H. Kroemer // *Appl. Phys. Lett.*, **60**, (1992) 3283.
18. R. Carles, N. Saint-Cricq, J.B. Renucci, A. Zwick // *Phys. Rev.*, **B22**, p. 4804 (1980).
19. See, e.g., M. Cardona, in Light Scattering in Solids II, edited by M. Cardona and G. Giintherodt (Springer, Berlin, 1982), p. 19.
20. T. Yuasa, M. Ishii // *Phys. Rev.*, **B37**, p. 7001 (1988).
21. D.A. Dahl, L.J. Sham // *Phys. Rew.*, **B16**, p. 51 (1977).
22. W.P. Chen, Y.J. Chen, E. Burstein // *Surf. Sci.*, **58**, p. 263 (1976).
23. S.J. Allen, Jr., D.C. Tsui, B. Vinter // *Sol. St. Comm.*, **20**, p. 425 (1976).
24. B. Jusserand, P. Voisin M. Voos, L.L. Chang, E.E. Mendez, L. Esaki // *Appl. Phys. Lett.*, **46**, p. 678 (1985).
25. J. Groenen, A. Mlayah, R. Carles // *Appl. Phys. Lett.*, **69**, p. 943 (1996).
26. J.M. Mattews, A.E. Blakeslee // *J. Cryst. Growth.*, **27**, p. 118 (1974).
27. I. Rasnik, M.J.S.P. Brasil, F. Cerdeira, C.A.C. Mendonca, M.A. Cotta // *J.Appl.Phys.*, **87**, p. 1165 (2000).
28. See, e.g., G. Abstreiter, M. Cardona, A. Pinczuk in Light Scattering in Solids IV, edited by M. Cardona and G. Giintherodt (Springer, Berlin, 1984), p. 12.
29. J. Spitzer, A. Hopner, M. Kuball, M. Cardona // *J. Appl. Phys.*, **77**, p. 811 (1995).
30. H. Kamioka, S. Saito, T. Suemoto // *J. Luminescence*, **87-89**, p. 923 (2000).
31. J. Tûmmler, J. Woitok, J. Hermans, J. Gerts, P. Scgneider, D. Moulin, M. Behet, K. Heime // *J. Cryst. Growth.*, **170**, p. 772 (1997).
32. S.G. Lyapin, P.C. Klipstein, N.J. Mason, P.J. Walker // *Superlatt. and Microstructures,* **15**, p. 499 (1994).
33. S.G. Lyapin, P.C. Klipstein, N.J. Mason, P.J. Walker // *Phys. Rev. Lett.*, **74**, p. 3285 (1995).
34. G.R. Booker, P.C. Klipstein, M. Lakrimi, S. Lyapin, N.J. Mason, I.J. Murgatroud, R.J. Nicholas, T.-Y. Seong, D.M. Symons, P.J. Walker // *J. Cryst. Growth.*, **146**, p. 495 (1995).